Published OnlineFirst August 16, 2010; DOI: 10.1158/0008-5472.CAN-10-0244

Cancer Research

FZD4 as a Mediator of *ERG* Oncogene–Induced WNT Signaling and Epithelial-to-Mesenchymal Transition in Human Prostate Cancer Cells

Santosh Gupta[1,2], Kristiina Iljin[1,2], Henri Sara[2], John Patrick Mpindi[4], Tuomas Mirtti[3], Paula Vainio[2], Juha Rantala[1], Kalle Alanen[3], Matthias Nees[1], and Olli Kallioniemi[1,2,4]

Abstract

TMPRSS2-ERG and other gene fusions involving ETS factors and genes with strong promoter elements are common in prostate cancer. Although *ERG* activation has been linked to invasive properties of prostate cancers, the precise mechanisms and pathways of *ERG*-mediated oncogenesis remain poorly understood. Here, we show that *ERG* knockdown in VCaP prostate cancer cells causes an activation of cell adhesion, resulting in strongly induced active β_1-integrin and E-cadherin expression as well as changes in WNT signaling. These observations were corroborated by data from *ERG*-overexpressing nontransformed prostate epithelial cells as well as gene expression data from clinical prostate cancer samples, which both indicated a link between *ERG* and epithelial-to-mesenchymal transition (EMT). Upregulation of several WNT pathway members was seen in *ERG*-positive prostate cancers, with frizzled-4 (*FZD4*) showing the strongest overexpression as verified by both reverse transcription-PCR and immunostaining. Both *ERG* knockin and knockdown modulated the levels of *FZD4* expression. *FZD4* silencing could mimic the *ERG* knockdown phenotype by inducing active β_1-integrin and E-cadherin expression, whereas *FZD4* overexpression reversed the phenotypic effects seen with *ERG* knockdown. Taken together, our results provide mechanistic insights to *ERG* oncogenesis in prostate cancer, involving activation of WNT signaling through *FZD4*, leading to cancer-promoting phenotypic effects, including EMT and loss of cell adhesion. *Cancer Res; 70(17); 6735–45. ©2010 AACR.*

Introduction

Gene fusions between the prostate-specific and androgen-responsive *TMPRSS2* gene and ETS transcription factors are found in roughly 50% of all prostate cancers. Most frequently, the fusion partner is *ERG* (ETS-related gene), followed by *ETV1, ETV4*, and *ETV5* (1–4). As a result of these oncogenic fusions, androgens and the androgen receptor (*AR*) signaling drive ETS factor overexpression, resulting in prostate cancer development and progression (5–7). *ERG* overexpression has also been described in acute myeloid leukemia and acute T-lymphoblastic leukemia, whereas the *EWS-ERG* gene fusion is characteristic to a subset of Ewing's sarcomas (8). High *ERG* expression is an independent risk factor in acute T-lymphoblastic leukemia predicting poor relapse-free survival (9, 10). *TMPRSS2-ERG* gene fusions occur early during prostate carcinogenesis. The fusion may have prognostic significance depending on the cytogenetic nature of the rearrangement, overexpression of the *ERG* gene, and disease stage (11–14).

The precise molecular events and signaling mechanisms contributing to *ERG*-initiated oncogenesis are incompletely understood. *ERG* has been shown to regulate invasion through the plasminogen activation pathway (15). The phenotypes in mouse models showed prostatic intraepithelial neoplasia formation, induction of β_4-integrin expression, and loss of stromal cells in prostates from transgenic mice with probasin promoter–driven *ERG* overexpression (15–17). Apparently, *ERG* overexpression in prostate epithelial cells is sufficient to induce neoplastic changes but not to produce carcinoma (15, 16). Coexpression of *AR* and *ERG* in mouse prostate epithelial cells induced invasive cancer with poorly formed, tightly packed prostate glands and loss of smooth muscle actin staining in stroma cells (17), suggesting that *AR* and *ERG* may act synergistically in the progression of PIN lesion to invasive adenocarcinoma. *ERG* is also associated with aberrant phosphoinositide 3-kinase pathway, which promotes prostate cancer progression (17). *ERG* overexpression in prostate tumor cells has been associated with induction of *C-MYC* and subsequent neoplastic changes (18). Finally, the results from our previous bioinformatics analyses of *ERG* coexpression in clinical prostate cancers suggest that *ERG* modulates epigenetic programming (19).

Authors' Affiliations: [1]Medical Biotechnology, VTT Technical Research Centre of Finland; [2]Turku Centre for Biotechnology and [3]Department of Pathology, University of Turku, Turku, Finland; and [4]Institute for Molecular Medicine Finland (FIMM), University of Helsinki, Helsinki, Finland

Note: Supplementary data for this article are available at Cancer Research Online (http://cancerres.aacrjournals.org/).

Corresponding Author: Olli Kallioniemi, Institute for Molecular Medicine Finland (FIMM), University of Helsinki and Medical Biotechnology, VTT Technical Research Centre of Finland, Itäinen Pitkäkatu 4, Turku, Finland. Phone: 358-40-5698192; Fax: 358-20-722-2840; E-mail: Olli.Kallioniemi@helsinki.fi.

doi: 10.1158/0008-5472.CAN-10-0244

©2010 American Association for Cancer Research.

Downloaded from cancerres.aacrjournals.org on April 10, 2021. © 2010 American Association for Cancer Research.

Published OnlineFirst August 16, 2010; DOI: 10.1158/0008-5472.CAN-10-0244

In this study, we examined the function of the *ERG* oncogene by knockdown and knockin experiments in prostate cell lines as well as carried out molecular pathologic analysis of *ERG*-positive clinical prostate cancers. We found that *ERG* silencing promotes cell adhesion and upregulates β_1-integrin and E-cadherin expression as well as WNT signaling. We then observed that frizzled-4 (*FZD4*) was often co-overexpressed with *ERG* in clinical prostate cancers and was systematically modulated by *ERG* manipulation *in vitro*. Silencing of *FZD4* mimicked the phenotypic effects seen with *ERG* knockdown, and *FZD4* overexpression reverted the phenotypic effects seen with *ERG* knockdown. These observations link *ERG* activation *in vitro* and in clinical prostate cancers with activation of the WNT pathway through *FZD4*, resulting in epithelial-to-mesenchymal transition (EMT) and changes in cell adhesion.

Materials and Methods

Patient data and prostate cancer cell lines

Sixteen localized prostate cancer samples were taken freshly from total prostatectomy specimen. The patients were not treated by any other modalities (radiation, hormonal therapy) with the subsequent knowledge on cancer grade. The study protocol was approved by the local ethical committee, and informed consent of the patients was obtained. Frozen tissue blocks were sectioned, and 4 to 6 μm sections were collected for DNA and RNA extractions. Clinical data of the patients are summarized in Supplementary Table S1. The immortalized prostate cell line RWPE1 and the *TMPRSS2-ERG* gene fusion–positive tumor cell line VCaP were obtained from the American Type Culture Collection and cultured in RPMI medium.

Generation of *GFP-ERG* and *GFP-FZD4* constructs

The full-length *ERG* cDNA was PCR amplified based on an open reading frame (ORF) clone purchased from Origene, Inc. (SC108516), by using *ERG* forward (5′-CAATCTCGAGCTATGGCCAGCACTATTAAGG AAGC-3′) and reverse (5′-CAATCCCGGGTTAGTAGTAAGTGCCCAGATGAGAAG-3′) primers with *Xho*I and *Xma*I restriction sites and Phusion High-Fidelity DNA polymerase (Finnzymes). The amplified cDNA was digested with *Xho*I and *Xma*I restriction enzymes, excised from agarose gels, and cloned into pEGFP-C1 (Invitrogen). Sequencing reactions using the same primers as in PCR were prepared by using the ABI BigDye Terminator V3.1 cycle sequencing kit and analyzed on the ABI 3100 genetic Analyzer (Applied Biosystems). The *FZD4-GFP* overexpression construct was ordered from Origene (RG217286). The pEGFP-*ERG* and pEGFP control vectors were transfected into RWPE1 cells by using the FuGENE-6 transfection reagent (Roche). RNA and protein samples were prepared 24, 48, and 72 hours after transfection. Harvested cells were used for RNA and protein isolation.

Western blot analysis

Cells were plated at 70% confluence and left to attach overnight. Protein content was measured using the Bio-Rad protein assay kit. Twenty micrograms of total protein were taken up in Laemmli buffer containing 3% of β-mercaptoethanol, denatured for 5 minutes at 95°C, separated on a 7% SDS-polyacrylamide gel, and transferred to a Protran nitrocellulose transfer membrane (Schleicher & Schuell). Green fluorescent protein (*GFP*; 1:1,000, rabbit polyclonal, A11122, Molecular probes), *ERG* (1:1,000, rabbit polyclonal, SC-353, Santa Cruz), and *FZD4* (1:1,000, goat polyclonal, SC-66450, Santa Cruz) antibodies were used for Western blotting. Antibody against *HSPA8* (heat shock 70 kDa protein 8, 1:1,000, rat monoclonal, SPA-815, Stressgen) was used as the loading control. Proteins from the cytosolic, membranous, and nuclear fractions were isolated using a Compartment Protein Extraction Kit (Chemicon) according to the manufacturer's instructions. The signal was detected with a 1:5,000 dilution of horseradish peroxidase (HRP)–conjugated anti-goat, anti-rat, or anti-rabbit secondary antibodies (Amersham ECL-HRP Linked Secondary Antibodies). ECL (GE Healthcare) Western Blotting Detection Systems was used for Western blot analysis.

siRNA and lentiviral shRNA knockdown of *ERG* in VCaP cells

The most effective siRNA against *ERG* (SI03089443, Qiagen; target all the isoforms of *ERG* gene), *FZD4* (SC-39983, Santa Cruz), or siCONTROL Non-Targeting siRNA (1027310, Qiagen) was transfected using the Lipofectamine 2000 reagent (Invitrogen) and tested for knockdown by quantitative reverse transcription-PCR (qRT-PCR) using the universal probe library (Roche). Samples were prepared after 24, 48, and 72 hours. To generate stable VCaP cells with reduced *ERG* mRNA expression, Mission *ERG* shRNA lentiviruses (NM_004449.3-2067s1c1, NM_004449.3-214s1c1 or 214, NM_004449.3-643s1c1 or 643, NM_004449.3-1404s1c1, and NM_004449.3-823s1c1) and Mission nontarget shRNA Lentiviral Particles (Mission/Sigma) with a titer of $>10^6$ TU/mL were used to infect VCaP cells. Subsequently, stable clones were selected using puromycin (2 μg/mL).

Fluorescence-activated cell sorting analysis

Twenty thousand cells per well were used for fluorescence-activated cell sorting (FACS) analysis of stable *ERG* 214 shRNA– and *FZD4* siRNA–treated VCaP cells as well as for the respective controls. A similar protocol was used for the analysis of *GFP-ERG*–, *GFP-FZD4*–, and *GFP*-transfected RWPE1 cells. Cells were trypsinized and fixed with 2% paraformaldehyde (PFA) with 0.5% Triton X-100 and resuspended in PBS. Cells were washed and stained with active β_1-integrin and E-cadherin (the same antibodies as those used in immunofluorescence staining; 1:1,500 dilutions) overnight at 4°C. After washings, cells were stained with Alexa 647–labeled secondary antibodies (1:2,000) for 1 hour at room temperature. Cells were washed and the mean fluorescence intensity was measured using Accuri C6 Flow Cytometer.

Cell adhesion assay

Plates (96 wells) were coated with laminin or fibronectin (0.50 μg/mL) overnight and blocked with 0.1% bovine serum

Downloaded from cancerres.aacrjournals.org on April 10, 2021. © 2010 American Association for Cancer Research.

Published OnlineFirst August 16, 2010; DOI: 10.1158/0008-5472.CAN-10-0244

albumin (BSA; 1 hour, 37°C). *ERG* siRNA and scrambled siRNA–transfected VCaP cells were harvested 72 hours after transfection. Trypsin was inactivated with 0.2% (wt/vol) soybean trypsin inhibitor (Sigma). Cells were suspended in 0.5% BSA in serum-free RPMI, seeded (5,000 cells per well) on the plates, and allowed to adhere for 30 minutes at 37°C. After washing with PBS, cells were fixed (4% PFA, 10 minutes) and stained with propidium iodide (PI). Adhesion was measured by counting the number of PI-stained cells using Acumen Assay Explorer (absorbance at 488 nm).

Real-time quantitative PCR analysis

Total cellular RNAs were isolated using the Trizol reagent. For cDNA synthesis, 100 ng of total RNA were reverse transcribed with the High Capacity cDNA Reverse Transcription kit (Applied Biosystems). qRT-PCR analysis was done on an Applied Biosystems 7900HT instrument, using specific primers designed by the Universal Human Probe Library Assay Design Center. Results were analyzed using SDS 2.3 and RQ manager software (Applied Biosystems), and the relative expression of mRNA was determined using β-actin as an endogenous control. Data are from two separate biological experiments, with triplicate samples. Primers are listed in Supplementary Table S2.

Illumina bead array expression profiling and bioinformatics analysis

Total RNA was isolated from *GFP* and *GFP-ERG*–transfected RWPE1 cells as well as from transfected *ERG* siRNA–, *ERG* 214 shRNA–, and *ERG* 643 shRNA–treated VCaP cells in duplicate. The integrity of the RNA was monitored before hybridization, using the Bioanalyzer 2100 (Agilent). Purified total RNA (500 ng) was amplified with the Total Prep Kit (Ambion), and the biotin-labeled cRNA was hybridized to Sentrix HumanRef-8 Expression Bead Chips (Illumina). The arrays were scanned with the Bead Array Reader. Raw Illumina data were processed using the R/Bioconductor software and the lumi package. Variance-stabilizing transformation and quantile normalization were applied as preprocessing steps and for background correction. Differential expression of genes from two independent biological replicates of each condition was identified by fitting a linear model for each gene using the limma package. For network analyses, data were uploaded into the MetaCore Analytical Suite version 2.0 (GeneGo). The raw data of the microarray analysis have been deposited in the GEO database (GSE16671).

Gene tissue index method

The gene tissue index (GTI) algorithm is comparable with the cancer outlier profile analysis (COPA) algorithm in detecting outliers (2). It is designed to lower the bias created by other outlier statistics that depend on the mean, mean absolute deviation, and outlier sums by normalizing the score based on the number of samples. A positive GTI score means that there are more outliers in the target group (e.g., cancer group) than in the reference group (e.g., normal group). A GTI score close to zero indicates no difference in the expression levels of that gene in the two groups.

Immunofluorescence and confocal microscopy

siRNA- and shRNA-treated cells were grown on coverslips in 24-well plates and fixed with 2% PFA in PBS, permeabilized with 0.5% Triton X-100 in fixative solution for 15 minutes at room temperature, rinsed in PBST (PBS, 0.01% Tween 20), and blocked with 20% horse serum for 60 minutes in a humidified chamber (1× PBS/0.05% NaN_3, 25 μL/coverslip). After fixing and blocking, coverslips were rinsed again in PBST and labeled with 25 μL primary antibody overnight. *FZD4*, active β_1-integrin (mouse, monoclonal, 12G10, Abcam), activation state–specific phosphor-epitope (20), and E-cadherin (mouse, monoclonal, ab1416, Abcam) primary antibodies (1:100 dilution) were used for immunostaining. The coverslips were washed and labeled with 25 μL of secondary antibodies conjugated with Alexa 488, Alexa 555, or Alexa 647 (1:500 dilution in PBST, Invitrogen) for 60 minutes. After PBST washes, coverslips were mounted with 3 μL Vectashield with 4′,6-diamidino-2-phenylindole (DAPI; H-1200, Vector Laboratories). A confocal laser scanning microscope (Axioplan 2 with LSM510) equipped with Plan-Apochromat 63×/1.4 oil objectives was used in imaging. Confocal images represent a single Z-section of 1 μm. Image J software was used to analyze the confocal images (21).

Immunohistochemical staining

Based on the qRT-PCR results, five *ERG*-positive and five *ERG*-negative prostate cancer samples as well as two normal prostate samples were selected for *FZD4* staining by immunohistochemistry. Frozen sections (6 μm thick) were cut to silan-coated glasses and dried at room temperature for 30 minutes, fixed at −20°C temperature with acetone for 10 minutes, and again dried for 10 minutes at room temperature. Slides were washed in Tris-buffered saline (TBS; pH 7.4–7.6) for 3 × 5 minutes. Endogenous peroxidase was blocked with 0.3% hydrogen peroxide in TBS for 20 minutes. Slides were washed and incubated in goat normal serum (15 μL goat normal serum in 1 mL TBS) for an hour in a moist chamber. Affinity-purified IgG to human *ERG* (1:100, rabbit polyclonal, Santa Cruz, SC-353) and *FZD4* (1:100, goat polyclonal, Santa Cruz, SC-66450) was diluted with 1% BSA in TBS and the slides were incubated with the primary antibody at 4°C overnight in a moist chamber. For the negative control, one slide in each staining procedure was incubated with rabbit normal serum (primary antibody omitted). After washing with TBS (3 × 5 min), the slides were incubated with biotinylated anti-goat secondary antibodies (in TBS-buffered 1% BSA) at room temperature, in a moist chamber, for 30 minutes. The slides were washed and incubated with Vectastain ABC reagent (Vector Laboratories) at room temperature in a moist chamber for 30 minutes. Slides were washed and stained with diaminobenzidine, counterstained with Mayer's hematoxylin, dehydrated, treated with xylene, and mounted.

T-cell factor/lymphoid enhancer factor reporter assay

The Cignal T-cell factor/lymphoid enhancer factor (*TCF/LEF*) reporter (*GFP*) assay kit (CCS-018G) was used to measure the activity of WNT signaling in prostate epithelial cells

Downloaded from cancerres.aacrjournals.org on April 10, 2021. © 2010 American Association for Cancer Research.

Published OnlineFirst August 16, 2010; DOI: 10.1158/0008-5472.CAN-10-0244

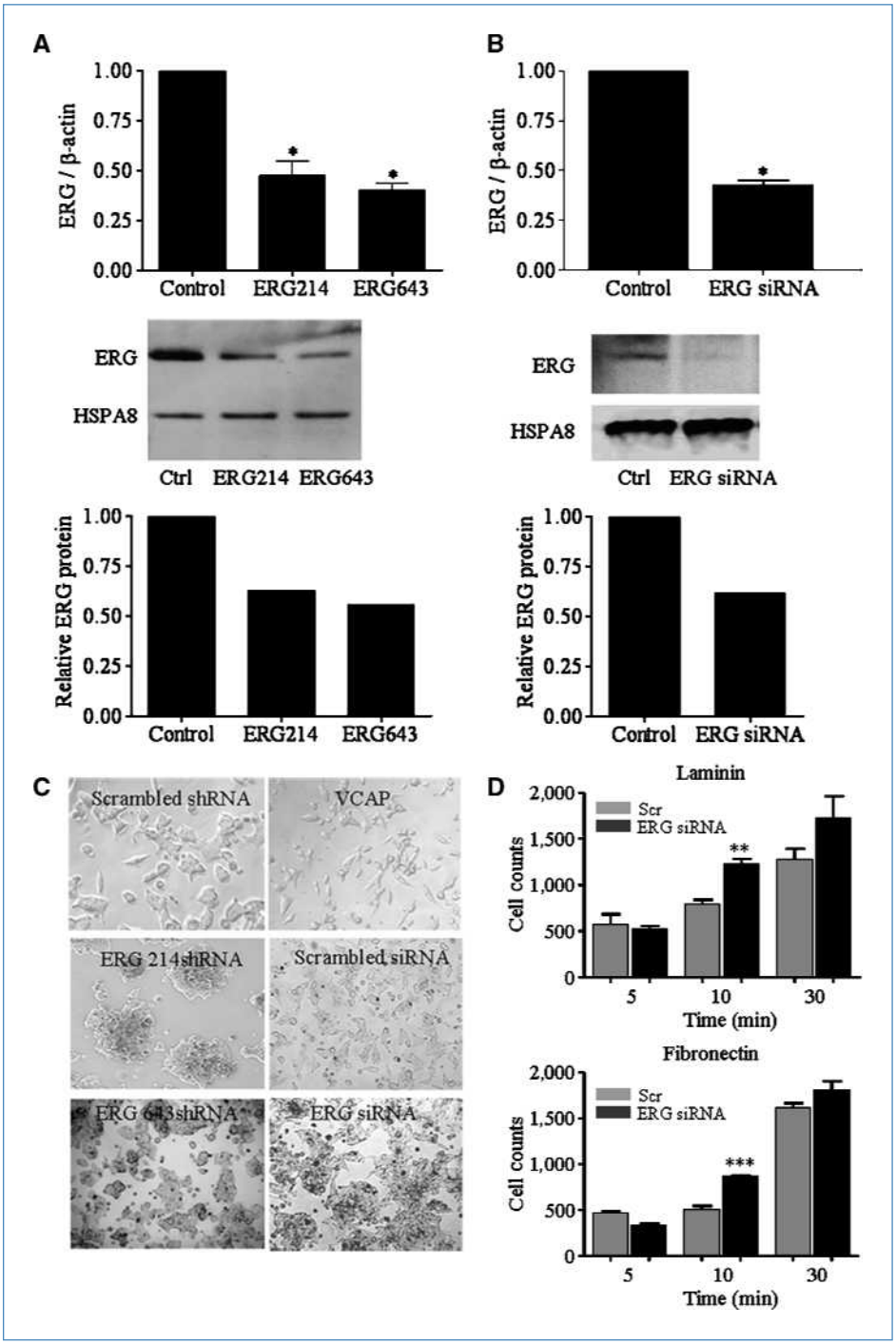

Figure 1. Validation of reduced *ERG* expression in *ERG* shRNA or siRNA-treated VCaP cells. A, qRT-PCR analysis, and Western blot analysis and its quantification to measure *ERG* expression in response to *ERG* silencing by stable expression of shRNA molecules (*ERG* 214 or 643) in VCaP cells. B, qRT-PCR analysis, and Western blot analysis and its quantification to measure *ERG* expression in response to *ERG* siRNA transfection at the 48 h time point in VCaP cells. To obtain the relative expression, *ERG* mRNA was normalized to β-actin mRNA (*, $P < 0.02$) and *ERG* protein was normalized to HSPA8. C, morphologic phenotype of scrambled shRNA–, *ERG* 214 shRNA–, and *ERG* 643 shRNA–expressing VCaP cells after puromycin selection, and scrambled siRNA– and *ERG* siRNA–treated VCaP cells 72 h after transfection. D, cell-cell adhesion analysis of *ERG* siRNA versus scrambled siRNA control in VCaP cells. siRNA-treated cells were allowed to attach on the laminin- or fibronectin-coated plates at different time points, and the PI-labeled cells were counted by using Acumen Explorer (**, $P < 0.005$; ***, $P < 0.001$).

in response to *ERG* modulation by using inducible *TCF/LEF*-responsive *GFP* reporter construct. Control *GFP* reporter was used to confirm the transfection efficiency. RWPE1 cells (20,000) were cultured in 96-well cluster plates and cotransfected with *GFP* or *GFP-ERG* overexpression construct (200 ng/well) together with *TCF/LEF* reporter construct (200 ng/well) for 48 and 72 hours. Similar experiments were done for *ERG* knockdown using both siRNA transfection– and stable shRNA expression–based approaches in VCaP cells. Also, *FZD4* siRNA–transfected VCaP cells were studied with appropriate scrambled controls at 48 and 72 hours. All transfections were done at least in triplicate, and *GFP* intensity was measured by Acumen Explorer. Graph Pad Prism 4 was used to plot the results and calculate the significance.

Downloaded from cancerres.aacrjournals.org on April 10, 2021. © 2010 American Association for Cancer Research.

Published OnlineFirst August 16, 2010; DOI: 10.1158/0008-5472.CAN-10-0244

Results

Silencing and overexpression of *ERG* in prostate cells

Five different shRNA lentiviral constructs were used to induce permanent knockdown of the *ERG* gene in VCaP cells that contain the *TMPRSS2-ERG* fusion gene (2, 22, 23). Selection with puromycin resulted in two stable cell lines with different *ERG* shRNAs (nos. 214 and 643). qRT-PCR and Western blot analyses (Fig. 1A) indicated 40% to 60% knockdown compared with a scrambled shRNA control. The partial knockdown efficacy may indicate that a more complete knockdown was not compatible with long-term cell survival. The *ERG* 214 shRNA cell line showed the most efficient reduction in *ERG* mRNA and was therefore subsequently used in functional experiments. Also, 10 different siRNAs targeting *ERG* were tested in transient transfection studies in VCaP cells, with those providing >50% knockdown chosen for further experiments (Fig. 1B). For overexpression studies, the full-length ORF for *ERG* was PCR amplified, cloned in-frame to enhanced *GFP* vector, and sequence verified. This construct and a control vector expressing only *GFP* were transfected into the immortalized, nonmalignant RWPE1 cells. The results indicate that the *GFP-ERG* fusion protein was almost exclusively nuclear whereas *GFP* localized to the cytoplasm (Supplementary Fig. S1A). Similar results were obtained by Western blot analysis of different subcellular protein fractions, indicating that the *GFP-ERG* fusion protein is effectively translocated into the nucleus (Supplementary Fig. S1B).

ERG silencing promotes cell adhesion by induction of active β_1-integrin and E-cadherin

Next, we explored phenotypic changes in VCaP prostate cancer cells in response to *ERG* knockdown either by stable shRNA or transient siRNA transfection. *ERG* shRNA– and *ERG* siRNA–transfected cells formed round cell clusters that were strongly adherent to culture plates (Fig. 1C). To confirm and quantitate the increased adhesion in response to *ERG* silencing, we performed cell adhesion assays using laminin and fibronectin matrix–coated plates at 5, 10, and 30 minutes time points. The results indicate that *ERG* siRNA silencing increased cell-cell adhesion compared with the scrambled

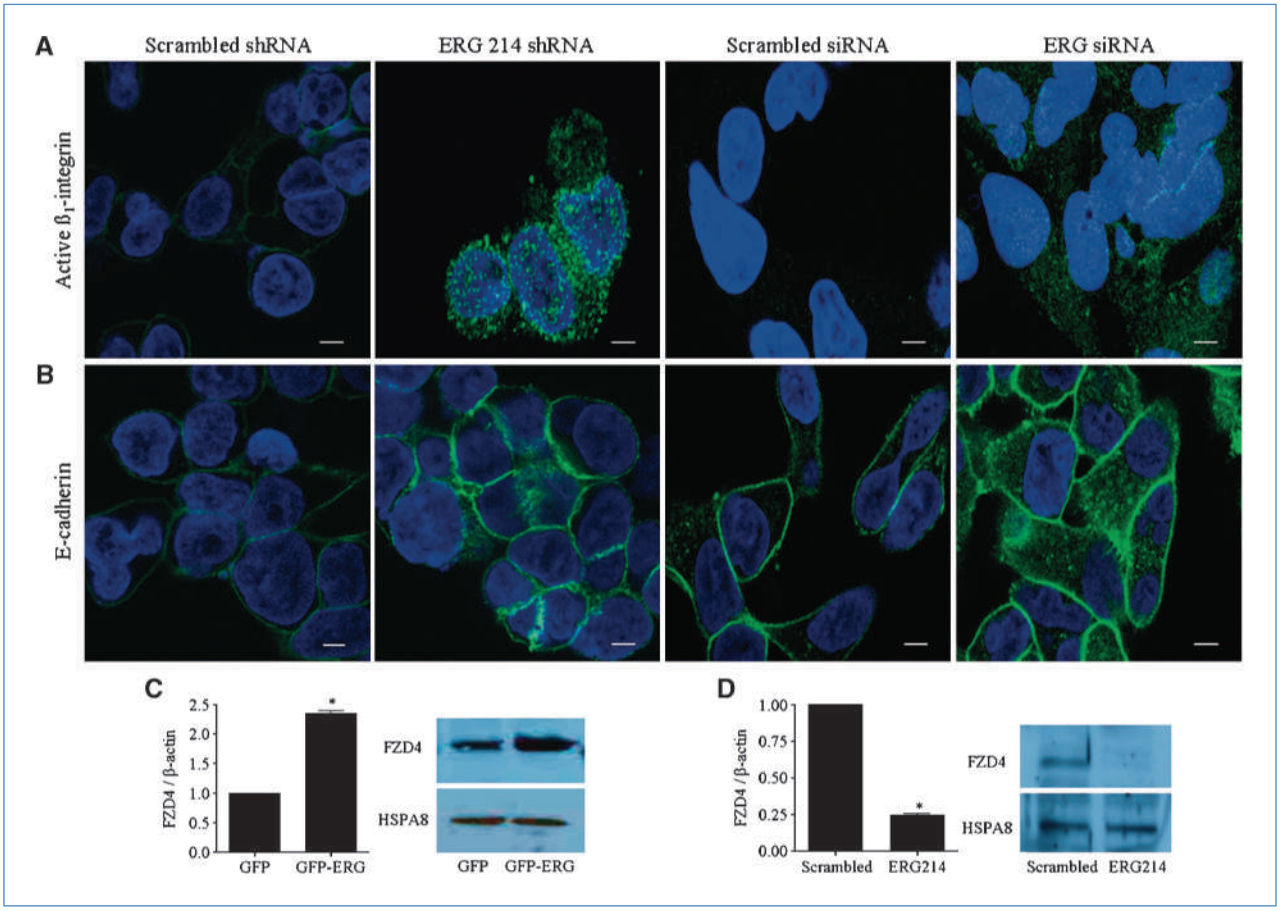

Figure 2. *ERG* silencing induces active β_1-integrin and E-cadherin expression. Immunostaining of stable scrambled shRNA and *ERG* 214 shRNA as well as scrambled siRNA and *ERG* siRNA exposed in VCaP cells was performed with antibodies against (A) active β_1-integrin and (B) E-cadherin. DAPI staining (blue) was used to visualize the nuclei. Taqman quantitative real-time PCR and Western blot analysis of (C) *FZD4* expression in RWPE1 cells transiently transfected with *GFP-ERG* vector and (D) stable *ERG* 214 shRNA–expressing VCaP cells with their respective control (*, $P < 0.05$).

Downloaded from cancerres.aacrjournals.org on April 10, 2021. © 2010 American Association for Cancer Research.

Published OnlineFirst August 16, 2010; DOI: 10.1158/0008-5472.CAN-10-0244

control (Fig. 1D). To study if this change was due to the differential expression of known regulators of cell attachment, VCaP cells with a stable *ERG* shRNA knockdown or transient *ERG* silencing were stained with antibodies against E-cadherin (*CDH1*) and active β_1-integrin and compared with the respective controls. *ERG* silencing induced strong active β_1-integrin (Fig. 2A) and E-cadherin (Fig. 2B) expression, which may explain the increased cell adhesion of VCaP cells in response to *ERG* knockdown. FACS analysis was performed to quantify the increased expression of active β_1-integrin and E-cadherin in response to *ERG* 214 shRNA–treated VCaP cells compared with the scrambled shRNA control cells. The results shown in Supplementary Fig. S2 indicate that *ERG* 214 shRNA significantly increased the expression of active β_1-integrin (>2-fold) and E-cadherin (>3.5-fold). These results support the earlier findings indicating increased invasion in response to *TMPRSS2-ERG* overexpression in prostate epithelial cells.

ERG modulation affects WNT signaling *in vitro*

To study the genome-wide consequences of *ERG* modulation, gene expression changes were measured by Illumina bead arrays in RWPE1 cells 48 to 72 hours after transfection of *GFP-ERG* compared with *GFP* only. Furthermore, these results were compared with data from transient *ERG* silencing in VCaP cells and with the stable VCaP cell lines expressing *ERG* shRNAs 214 or 643, all with the respective controls. We listed the top differentially expressed genes in response to *ERG* modulation as Supplementary Tables S3 and S4. The WNT pathway was one of the most systematically altered signaling pathways in the *ERG* modulation experiments according to bioinformatics analysis by gene set enrichment analysis and MetaCore and GeneGo pathway analyses (Supplementary Table S5). For example, in the *ERG-GFP*–transfected cells, the genes implicated in WNT signaling were *FZD4* and disabled homologue 2 (*DAB2*; both upregulated) and dickkopf homologue 1 (*DKK1*; downregulated).

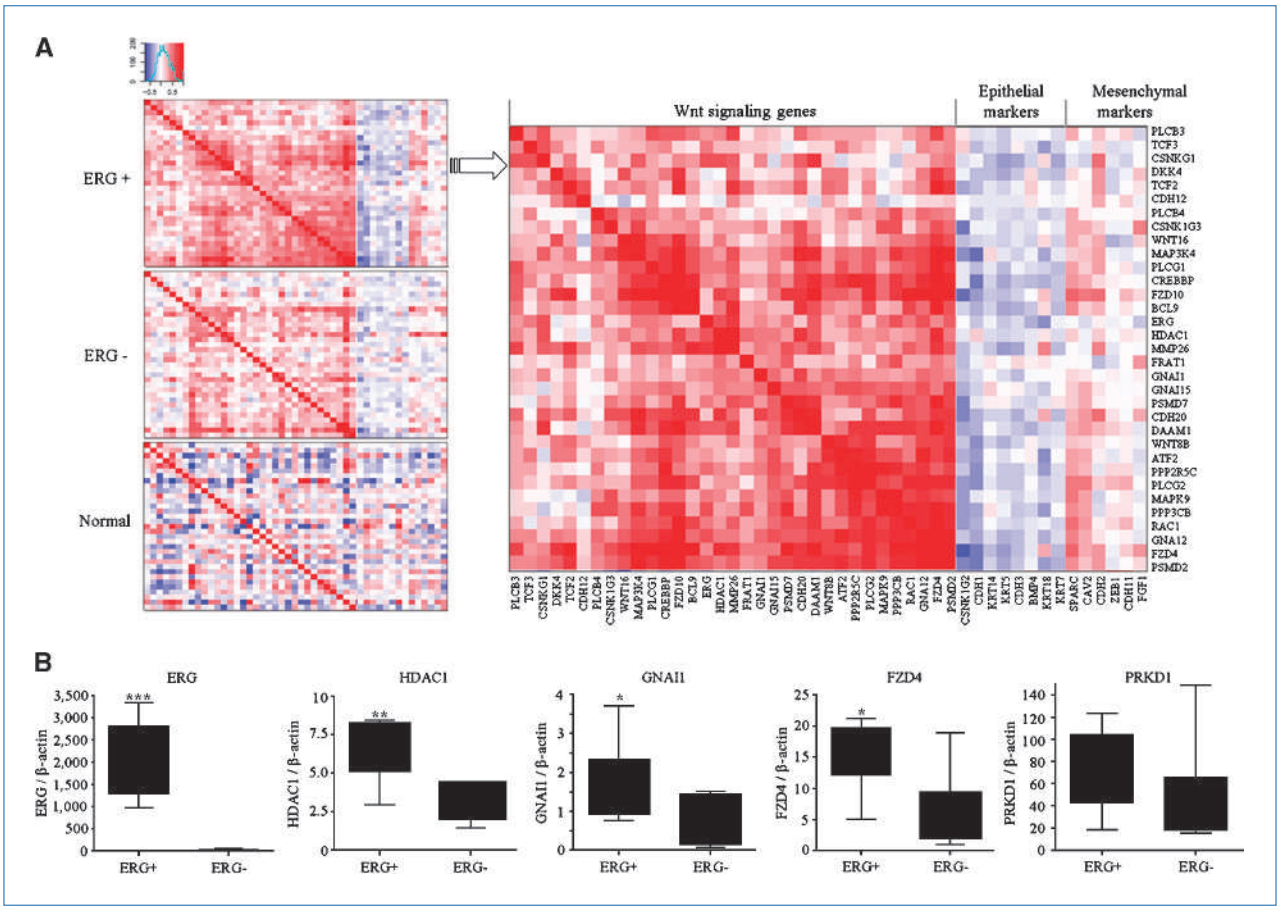

Figure 3. Coexpression analysis of WNT signaling genes in prostate tissues. A, coexpression analysis of WNT signaling genes in *ERG*-positive and *ERG*-negative prostate cancers as well as in normal prostate. Red areas indicate strong, positive correlation between genes; blue areas indicate negative correlation or anticorrelation. The map indicates increased correlation between the WNT pathway genes in *ERG*-positive tumors, less correlation in *ERG*-negative tumors, and no correlation in normal prostate tissues. The expression of epithelial and mesenchymal marker genes is shown for reference to visualize the association of induced WNT signaling with EMT. B, validation of increased expression of WNT genes in *ERG*-positive prostate cancers: The top five genes, *HDAC1* (**, $P < 0.001$), *GNAI1* (*, $P < 0.03$), *FZD4* (*, $P < 0.01$), and *PRKD1*, were significantly upregulated in *ERG*-positive ($n = 9$) compared with *ERG*-negative ($n = 7$) prostate cancers. All experiments were done in triplicates.

Downloaded from cancerres.aacrjournals.org on April 10, 2021. © 2010 American Association for Cancer Research.

Published OnlineFirst August 16, 2010; DOI: 10.1158/0008-5472.CAN-10-0244

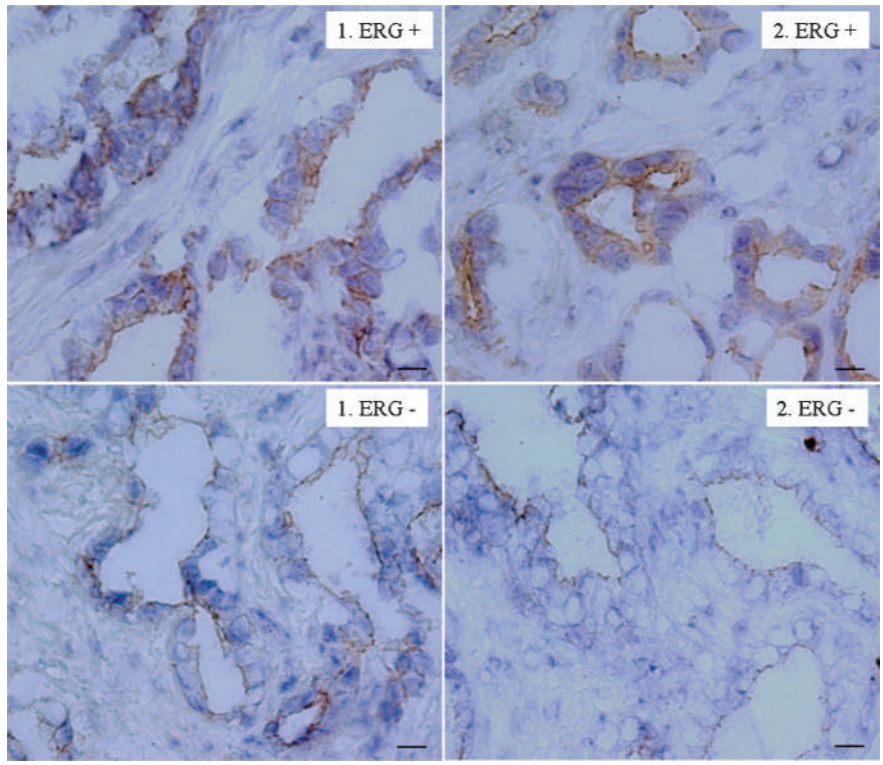

Figure 4. Immunohistochemical staining of *FZD4* in clinical prostate tumors. *ERG*-positive cancer samples (tumors 217O and 241V with Gleason grades 4 and 3) showed intense membrane-bound *FZD4* staining in carcinoma cells, whereas *ERG*-negative cancers (tumors 350O and 224V with Gleason grades 4 and 5) showed weak *FZD4* expression in epithelial cell membranes.

In contrast, axin-related protein (*AXIN2*); lymphoid enhancer binding factor-1 (*LEF1*); and protein phosphatase 1, catalytic subunit, β isoform (*PPP1CB*) were all upregulated in the permanent *ERG*-shRNA knockdown cell line variants. On the other hand, *FZD4* and plasminogen activator and urokinase receptor (*PLAUR*) were downregulated.

FZD4, a WNT receptor, was one of the most consistently differentially expressed genes in response to both *ERG* knockdown and upregulation in human prostate cells. We confirmed a relationship between *FZD4* and *ERG* by qRT-PCR in *ERG*-overexpressing RWPE1 cells and in the stable *ERG* 214 shRNA–expressing VCaP cells. The results indicate that *ERG* overexpression increased *FZD4* expression whereas *ERG* silencing resulted in decreased *FZD4* at both the mRNA and protein levels (Fig. 2C and D).

Coexpression of WNT signaling genes in *ERG*-positive prostate cancers

To explore the relationship between *ERG* and the WNT pathway *in vivo* in clinical prostate cancer specimens, a systematic bioinformatics analysis of genes involved in the WNT pathway was performed. We identified 226 WNT pathway genes from the Biocompare database (http://gspd.biocompare.com/). The GeneSapiens gene expression database (http://www.genesapiens.org) was used to identify those that had both an outlier expression in prostate cancer and were positively correlated with the *ERG* oncogene expression (24) in 70 *ERG*-positive and 267 *ERG*-negative prostate cancer samples compared with samples from 159 nonmalignant prostates. A correlation value >0.3 ($P < 0.05$) with *ERG* and a positive GTI outlier score in *ERG*-positive samples were used for selecting genes to explore in a coexpression network.[5] The results are shown in Supplementary Table S6. In accordance with our previous study (19), histone deacetylase inhibitor 1 (*HDAC1*) showed the highest association with *ERG*-positive prostate cancers. *FZD4*, identified as an ERG-modulated gene in functional experiments with prostate epithelial cells, was among the top WNT pathway outlier genes correlating with *ERG*.

We then studied the coexpression patterns of *ERG*, WNT-pathway genes, and markers for epithelial and mesenchymal differentiation in the 496 prostate tissue samples. The expression data presented as a correlation map (Fig. 3A) indicate that *ERG* mRNA correlated with WNT pathway activation, increased expression of mesenchymal markers such as cadherins *CDH2* and *CDH11*, and reduced expression of epithelial markers such as the luminal keratins *KRT7* and *KRT18*. To find out if EMT-regulating transcription factors are differentially expressed in response to *ERG* modulation, *SNAI1* and *SNAI2* mRNA expression were studied. The results are shown in Supplementary Fig. S3 and indicate that *ERG*

[5] Mpindi et al. Bioinformatics (Oxford University Press), submitted for publication.

Downloaded from cancerres.aacrjournals.org on April 10, 2021. © 2010 American Association for Cancer Research.

Published OnlineFirst August 16, 2010; DOI: 10.1158/0008-5472.CAN-10-0244

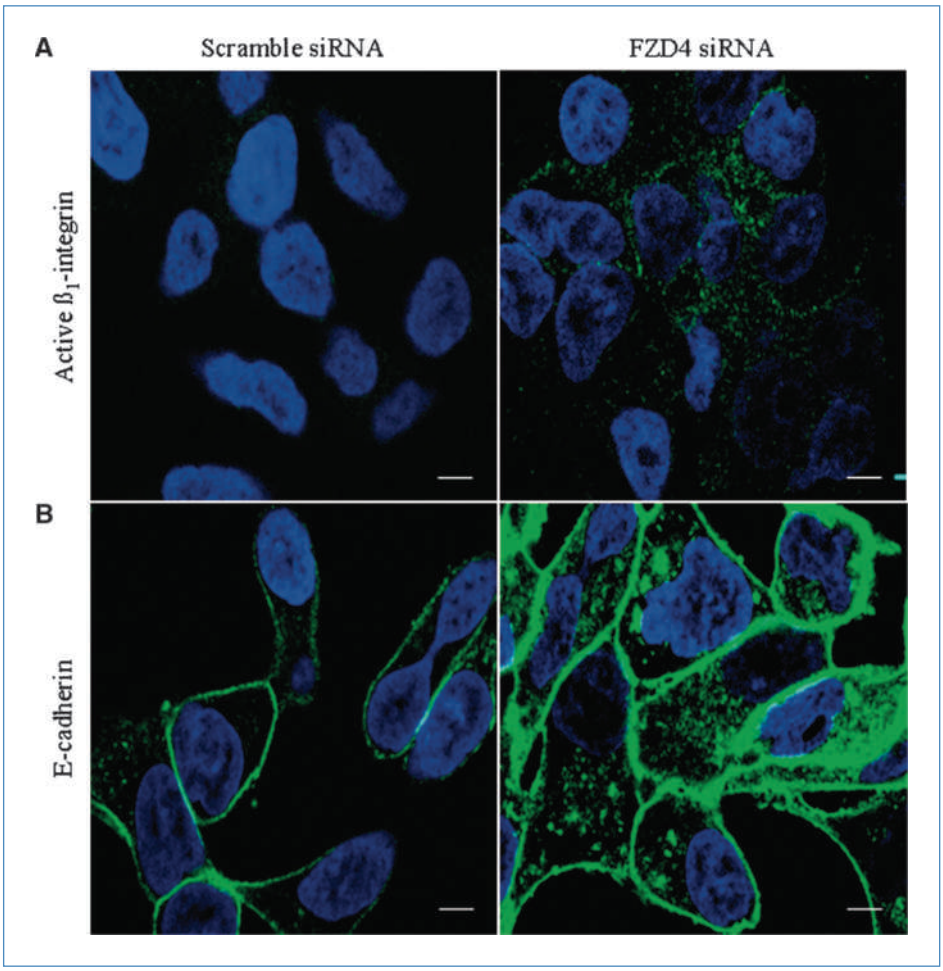

Figure 5. Immunostaining of active β_1-integrin and E-cadherin in response to *FZD4* silencing in VCaP cells. Immunostaining of scrambled siRNA– and *FZD4* siRNA–treated VCaP cells with antibodies against (A) active β_1-integrin and (B) E-cadherin (green) after 48 hours transfection.

silencing reduced *SNAI1* and *SNAI2* expression in VCaP cells, whereas increased *SNAI1* mRNA was seen in response to *ERG* overexpression in RWPE1 cells. These results are in accordance with the profiles we observed in the *in vitro* functional experiments and support the role of *ERG* in regulating WNT signaling and activation of EMT.

Validation of WNT pathway activation and *FZD4* in *ERG*-positive clinical samples

We validated the expression levels of 15 *ERG* coexpressed genes, including several genes involved in WNT signaling, by qRT-PCR in nine *ERG*-positive and seven *ERG*-negative prostate cancer samples. The results confirmed that *HDAC1*, guanine nucleotide binding protein (G protein), α inhibiting activity polypeptide 1 (*GNAI1*), *FZD4*, and protein kinase D1 (*PRKD1*) were highly correlated with *ERG* in clinical prostate samples (Fig. 3B). For some genes, associations may link these to other central signaling molecules important for prostate cancer progression. For example, protein kinase D1 (*PRKD1*), which is upregulated in *ERG*-positive prostate cancer, interacts with E-cadherin, which is dysregulated in prostate cancer and associated with altered cell aggregation and motility (25). *FZD4* was also analyzed immunohistochemically in frozen sections derived from the same clinical prostate cancer samples used in qRT-PCR experiments. There was a trend toward higher *FZD4* protein expression in *ERG*-positive tumors compared with *ERG*-negative samples (Fig. 4). *FZD4* protein was predominantly membrane bound and associated with cancer cells.

FZD4 silencing induces active β_1-integrin and E-cadherin expression

To explore the role of *FZD4* in cell-cell contacts and in cell adhesion, we knocked down *FZD4* by siRNA in VCaP cells and confirmed by qRT-PCR, Western blot, and immunostaining (Supplementary Fig. S4). *FZD4* silencing resulted in upregulation of active β_1-integrin (Fig. 5A) and E-cadherin (Fig. 5B) expression in VCaP cells in an identical way as observed for *ERG* knockdown and also confirmed by FACS by using labeled active β_1-integrin and E-cadherin antibodies (Supplementary Fig. S5A and B). Similar FACS analysis was performed with *GFP-ERG*– and *GFP-FZD4*–transfected VCaP cells at the 72-hour time point. The results indicate that *GFP-ERG* and *GFP-FZD4* overexpression reduced active β_1-integrin and E-cadherin expression (Supplementary Fig. S5C and D). This supports the idea

Downloaded from cancerres.aacrjournals.org on April 10, 2021. © 2010 American Association for Cancer Research.

Published OnlineFirst August 16, 2010; DOI: 10.1158/0008-5472.CAN-10-0244

that *FZD4* is sufficient to mediate the effects of *ERG* on EMT and cell adhesion in prostate cancer cells.

FZD4 as a critical regulator of WNT signaling in *ERG*-positive prostate cancer

To assess the activation of WNT signaling in response to *ERG* overexpression, *TCF/LEF GFP* Reporter Assay was performed in *GFP-ERG*–transfected RWPE1 cells at 48 and 72 hours. The results are shown in Fig. 6A and indicate a 2.4-fold higher WNT signaling in response to *ERG* overexpression. Moreover, the activity of the WNT pathway was 3-fold reduced by *ERG* knockdown, as evaluated by comparison of *TCF/LEF* reporter activity in stable *ERG* 214 shRNA–expressing VCaP cells with scrambled shRNA control cells (Fig. 6B). Transient silencing of *ERG* by siRNA transfection in VCaP cells also resulted in reduced *TCF/LEF* reporter activity in accordance with *ERG* shRNA knockdown results. As expected based on the role of the *FZD4* gene in the WNT pathway, *FZD4* siRNA knockdown reduced the *TCF/LEF* reporter activity in VCaP cells (Fig. 6C). To validate our hypothesis that *FZD4* mediates the effect of *ERG*, we overexpressed *FZD4* in VCaP cells and simultaneously performed *ERG* silencing using siRNAs. The results indicate that *FZD4* overexpression reversed the effect of *ERG* knockdown on WNT activity in VCaP cells (Fig. 6D).

Discussion

Knockdown of *ERG* in the *TMPRSS2-ERG* fusion–positive VCaP prostate cancer cells resulted in clusters of strongly adherent cells with induction of active β_1-integrin and E-cadherin expression. Increased *ERG* activity in turn was associated with EMT, evidenced as both repression of epithelial-specific genes, such as E-cadherin and cytokeratins, and increased expression of mesenchymal-specific genes, such as *CDH2* and *CDH11*. Loss of E-cadherin is a hallmark of EMT, a process implicated in aggressive tumor cell behavior, invasion, and metastasis (26–29). Our results indicate that *ERG* represses E-cadherin expression, by inducing Snail transcription factors, central players in EMT transitions. In addition, increased cell adhesion accompanied with induced active β_1-integrin expression may indicate reduced motile/invasive behavior of the tumor cells in response to *ERG* silencing because decrease in β_1-integrin expression has been linked to increased invasion in prostate cancer cells (30). Interestingly, *ERG* overexpression in prostate cells has been shown to increase invasion in RWPE 1 and silencing of activated *ERG* to reduce invasion in VCaP cells (15). Taken together, our data suggest that this effect is primarily mediated by EMT accompanied with profound changes in cell adhesion. The integrated evidence from both *ERG* manipulation *in vitro* and gene coexpression studies in clinical tumors indicated activation of the WNT pathway, and in particular overexpression of the *FZD4* gene, in *ERG*-positive tumors. *FZD4* silencing mimicked the *ERG* knockdown phenotype by also inducing active β_1-integrin and E-cadherin expression. Furthermore, *FZD4* overexpression reversed the impact of *ERG* knockdown in prostate cancer cells. These results suggest that in VCaP cells, *FZD4* is both necessary and sufficient as a mediator of the oncogenic effects of *ERG* overexpression. The association between *ERG* and *FZD4* gene expression in clinical specimens suggests that

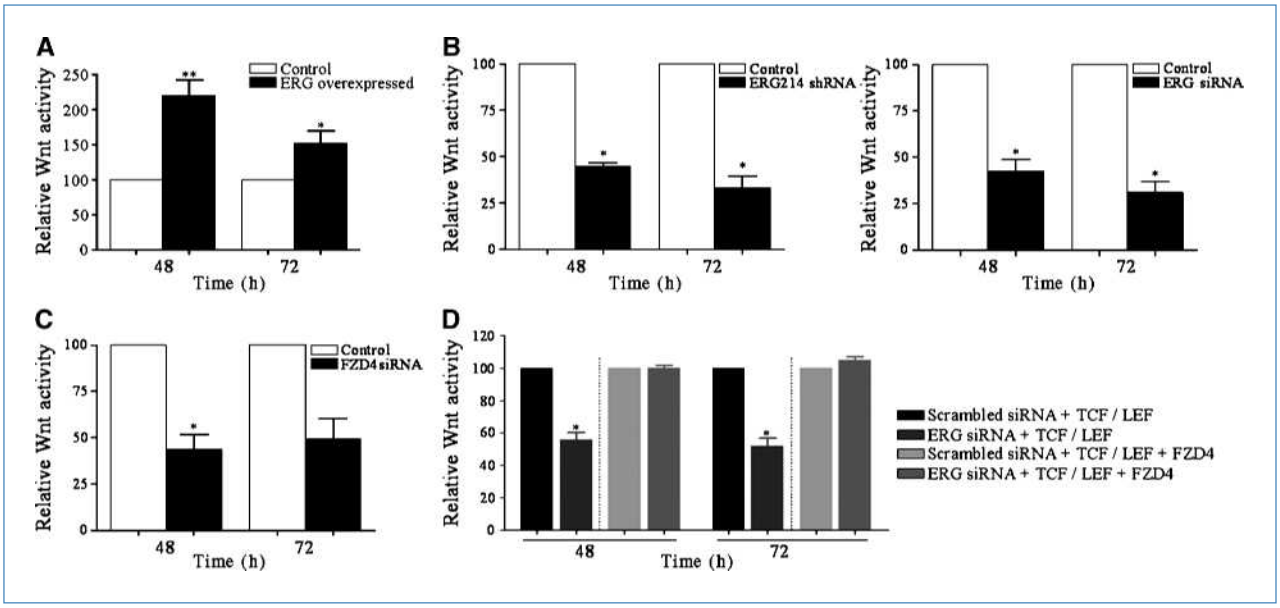

Figure 6. *TCF/LEF* reporter assay: *ERG* and *FZD4* regulates WNT signaling. WNT activity was measured by Acumen Explorer by using inducible *TCF/LEF* reporter (*GFP*) at different time points. A, RWPE1 cells were cotransfected with *TCF/LEF* reporter and *GFP-ERG* or *GFP* vector followed by WNT activity measurement at the 48 and 72 h time points. B, WNT activity in *ERG*-silenced VCaP cells by shRNA and siRNA compared with the respective controls. C, WNT activity in *FZD4* siRNA–treated VCaP cells. D, WNT activity was rescued by *FZD4* overexpression in *ERG* siRNA–treated VCaP cells (*, $P < 0.05$; **, $P < 0.001$).

Downloaded from cancerres.aacrjournals.org on April 10, 2021. © 2010 American Association for Cancer Research.

Published OnlineFirst August 16, 2010; DOI: 10.1158/0008-5472.CAN-10-0244

such a mechanism of oncogenesis may be operational *in vivo* as well. The detected mRNA and protein expression changes in clinical prostate cancer samples indicate that EMT is a relatively early change in carcinogenesis, and *FZD4* overexpression (31) could be driven by the downstream effects of the *ERG*-fusion gene.

Our study therefore provides novel insights into the critical pathways by which ectopic *ERG* oncogene expression may initiate and promote prostate cancer progression. In particular, we provide evidence to support the hypothesis that *ERG*-mediated oncogenesis in prostate cancer involves activation of WNT signaling through *FZD4*, leading to key cancer-promoting phenotypic effects, such as EMT and loss of cell adhesion. Our preliminary results also indicate that an experimental WNT pathway inhibitor, 4-(chloromethyl)benzoyl chloride, reduced the growth of the *ERG*-positive VCaP prostate cancer cells more efficiently than that of *ERG*-negative RWPE1 prostate cells.[6] This suggests that in exploring specific treatment strategies for *ERG*-positive prostate cancer patients, it may be possible to target downstream signaling events, such as WNT signaling (32).

[6] S. Gupta et al., unpublished data.

Disclosure of Potential Conflicts of Interest

No potential conflicts of interest were disclosed.

Acknowledgments

We thank the Finnish DNA Microarray Centre for performing TaqMan qRT-PCR analysis.

Grant Support

Academy of Finland Center of Excellence program, Sigrid Juselius Foundation, Finnish Cancer Society, and EU-FP7 Epitron.

The costs of publication of this article were defrayed in part by the payment of page charges. This article must therefore be hereby marked *advertisement* in accordance with 18 U.S.C. Section 1734 solely to indicate this fact.

Received 01/21/2010; revised 06/17/2010; accepted 06/30/2010; published OnlineFirst 08/16/2010.

References

1. Helgeson BE, Tomlins SA, Shah N, et al. Characterization of TMPRSS2:ETV5 and SLC45A3:ETV5 gene fusions in prostate cancer. Cancer Res 2008;68:73–80.
2. Tomlins SA, Rhodes DR, Perner S, et al. Recurrent fusion of TMPRSS2 and ETS transcription factor genes in prostate cancer. Science 2005;310:644–8.
3. Tomlins SA, Mehra R, Rhodes DR, et al. TMPRSS2:ETV4 gene fusions define a third molecular subtype of prostate cancer. Cancer Res 2006;66:3396–400.
4. Tomlins SA, Mehra R, Rhodes DR, et al. Integrative molecular concept modeling of prostate cancer progression. Nat Genet 2007;39:41–51.
5. Hermans KG, van Marion R, van Dekken H, Jenster G, van Weerden WM, Trapman J. TMPRSS2:ERG fusion by translocation or interstitial deletion is highly relevant in androgen-dependent prostate cancer, but is bypassed in late-stage androgen receptor-negative prostate cancer. Cancer Res 2006;66:10658–63.
6. Mehra R, Tomlins SA, Shen R, et al. Comprehensive assessment of TMPRSS2 and ETS family gene aberrations in clinically localized prostate cancer. Mod Pathol 2007;20:538–44.
7. Perner S, Mosquera JM, Demichelis F, et al. TMPRSS2-ERG fusion prostate cancer: an early molecular event associated with invasion. Am J Surg Pathol 2007;31:882–8.
8. Giovannini M, Biegel JA, Serra M, et al. EWS-erg and EWS-Fli1 fusion transcripts in Ewing's sarcoma and primitive neuroectodermal tumors with variant translocations. J Clin Invest 1994;94:489–96.
9. Marcucci G, Mrozek K, Bloomfield CD. Molecular heterogeneity and prognostic biomarkers in adults with acute myeloid leukemia and normal cytogenetics. Curr Opin Hematol 2005;12:68–75.
10. Baldus CD, Burmeister T, Martus P, et al. High expression of the ETS transcription factor ERG predicts adverse outcome in acute T-lymphoblastic leukemia in adults. J Clin Oncol 2006;24:4714–20.
11. Attard G, Clark J, Ambroisine L, et al. Duplication of the fusion of TMPRSS2 to ERG sequences identifies fatal human prostate cancer. Oncogene 2008;27:253–63.
12. Hermans KG, Boormans JL, Gasi D, et al. Overexpression of prostate-specific TMPRSS2(exon 0)-ERG fusion transcripts corresponds with favorable prognosis of prostate cancer. Clin Cancer Res 2009;15:6398–403.
13. Tu JJ, Rohan S, Kao J, Kitabayashi N, Mathew S, Chen YT. Gene fusions between TMPRSS2 and ETS family genes in prostate cancer: Frequency and transcript variant analysis by RT-PCR and FISH on paraffin-embedded tissues. Mod Pathol 2007;20:921–8.
14. Wang J, Cai Y, Ren C, Ittmann M. Expression of variant TMPRSS2/ERG fusion messenger RNAs is associated with aggressive prostate cancer. Cancer Res 2006;66:8347–51.
15. Tomlins SA, Laxman B, Varambally S, et al. Role of the TMPRSS2-ERG gene fusion in prostate cancer. Neoplasia 2008;10:177–88.
16. Klezovitch O, Risk M, Coleman I, et al. A causal role for ERG in neoplastic transformation of prostate epithelium. Proc Natl Acad Sci U S A 2008;105:2105–10.
17. Zong Y, Xin L, Goldstein AS, Lawson DA, Teitell MA, Witte ON. ETS family transcription factors collaborate with alternative signaling pathways to induce carcinoma from adult murine prostate cells. Proc Natl Acad Sci U S A 2009;106:12465–70.
18. Sun C, Dobi A, Mohamed A, et al. TMPRSS2-ERG fusion, a common genomic alteration in prostate cancer activates C-MYC and abrogates prostate epithelial differentiation. Oncogene 2008;27:5348–53.
19. Iljin K, Wolf M, Edgren H, et al. TMPRSS2 fusions with oncogenic ETS factors in prostate cancer involve unbalanced genomic rearrangements and are associated with HDAC1 and epigenetic reprogramming. Cancer Res 2006;66:10242–6.
20. Mould AP, Askari JA, Barton S, et al. Integrin activation involves a conformational change in the α1 helix of the β subunit A-domain. J Biol Chem 2002;277:19800–5.
21. Collins TJ. ImageJ for microscopy. BioTechniques 2007;43:25–30.
22. Perner S, Demichelis F, Beroukhim R, et al. TMPRSS2:ERG fusion-associated deletions provide insight into the heterogeneity of prostate cancer. Cancer Res 2006;66:8337–41.
23. Demichelis F, Fall K, Perner S, et al. TMPRSS2:ERG gene fusion associated with lethal prostate cancer in a watchful waiting cohort. Oncogene 2007;26:4596–9.
24. Kilpinen S, Autio R, Ojala K, et al. Systematic bioinformatic analysis of expression levels of 17,330 human genes across 9,783 samples from 175 types of healthy and pathological tissues. Genome Biol 2008;9:R139.
25. Syed V, Mak P, Du C, Balaji KC. β-Catenin mediates alteration in cell proliferation, motility and invasion of prostate cancer cells by differential expression of E-cadherin and protein kinase D1. J Cell Biochem 2008;104:82–95.

Downloaded from cancerres.aacrjournals.org on April 10, 2021. © 2010 American Association for Cancer Research.

Published OnlineFirst August 16, 2010; DOI: 10.1158/0008-5472.CAN-10-0244

26. Margineanu E, Cotrutz CE, Cotrutz C. Correlation between E-cadherin abnormal expressions in different types of cancer and the process of metastasis. Rev Med Chir Soc Med Nat Iasi 2008;112:432–6.

27. Schmalhofer O, Brabletz S, Brabletz T. E-cadherin, β-catenin, and ZEB1 in malignant progression of cancer. Cancer Metastasis Rev 2009;28:151–66.

28. Peinado H, Olmeda D, Cano A. Snail, zeb and bHLH factors in tumour progression: an alliance against the epithelial phenotype? Nat Rev Cancer 2007;7:415–28.

29. Brabletz T, Hlubek F, Spaderna S, et al. Invasion and metastasis in colorectal cancer: Epithelial-mesenchymal transition, mesenchymal-epithelial transition, stem cells and β-catenin. Cells Tissues Organs 2005;179:56–65.

30. Dedhar S, Saulnier R, Nagle R, Overall CM. Specific alterations in the expression of $\alpha_3\beta_1$ and $\alpha_6\beta_4$ integrins in highly invasive and metastatic variants of human prostate carcinoma cells selected by *in vitro* invasion through reconstituted basement membrane. Clin Exp Metastasis 1993;11:391–400.

31. Acevedo VD, Gangula RD, Freeman KW, et al. Inducible FGFR-1 activation leads to irreversible prostate adenocarcinoma and an epithelial-to-mesenchymal transition. Cancer Cell 2007;12:559–71.

32. Barker N, Clevers H. Mining the wnt pathway for cancer therapeutics. Nat Rev Drug Discov 2006;5:997–1014.

Downloaded from cancerres.aacrjournals.org on April 10, 2021. © 2010 American Association for Cancer Research.

Published OnlineFirst August 16, 2010; DOI: 10.1158/0008-5472.CAN-10-0244

AACR American Association for Cancer Research

Cancer Research

The Journal of Cancer Research (1916–1930) | The American Journal of Cancer (1931–1940)

FZD4 as a Mediator of *ERG* Oncogene –Induced WNT Signaling and Epithelial-to-Mesenchymal Transition in Human Prostate Cancer Cells

Santosh Gupta, Kristiina Iljin, Henri Sara, et al.

Cancer Res 2010;70:6735-6745. Published OnlineFirst August 16, 2010.

Updated version	Access the most recent version of this article at: doi:10.1158/0008-5472.CAN-10-0244
Supplementary Material	Access the most recent supplemental material at: http://cancerres.aacrjournals.org/content/suppl/2010/08/13/0008-5472.CAN-10-0244.DC1

Cited articles	This article cites 32 articles, 12 of which you can access for free at: http://cancerres.aacrjournals.org/content/70/17/6735.full#ref-list-1
Citing articles	This article has been cited by 24 HighWire-hosted articles. Access the articles at: http://cancerres.aacrjournals.org/content/70/17/6735.full#related-urls

E-mail alerts	Sign up to receive free email-alerts related to this article or journal.
Reprints and Subscriptions	To order reprints of this article or to subscribe to the journal, contact the AACR Publications Department at pubs@aacr.org.
Permissions	To request permission to re-use all or part of this article, use this link http://cancerres.aacrjournals.org/content/70/17/6735. Click on "Request Permissions" which will take you to the Copyright Clearance Center's (CCC) Rightslink site.

Downloaded from cancerres.aacrjournals.org on April 10, 2021. © 2010 American Association for Cancer Research.